TERNARY INTERDIFFUSION COEFFICICENTS IN α2 - PHASE Ti3Al/Nb SYSTEM

W. Wang*, B. Yuan*, C. Zhou*,

*Key Laboratory of Aerospace Materials and Performance (Ministry of Education), School of Materials Science and Engineering, Beihang University, 37 Xueyuan Rd., Beijing 100191, China

Abstract

The α_2 single phase interdiffusion in Ti_3Al-Nb ternary system was studied at temperatures of 1323, 1373 and 1423 K. The interdiffusion coefficients were calculated by the method of Dayananda. The average ternary interdiffusion coeffcients were determined in the mid of the diffusion zone, and the trace diffusion coefficients can be estimitaed in the limit $c_X \to 0$. The obtained main interdiffusion coeffcients is little smaller than pivious reported and the diffusion activation energy of Nb calculated by the trace diffusion coefficients is 299.29 kJmol^{-1} accoding to the Arrhenius equation. These results can provide a theoretical basis for the mechanisms of Nb improving the oxidation resistance of Ti_3Al.

Keywords: Oxidation; Diffusion; Interdiffusion; Ti_3Al-Nb

1. Introduction

In aerospace and gas turbine industries, Ti-Al based alloys exhibit several potential applications, in which Ti_3Al are attractive materials for their outstanding properties, such as low density, intrinsic strength retention, high stiffness, high melting point and creep resistance. Unfortunately, oxidation resistance in the actual service is considerably inferior to that of other excellent superalloys [1-3]. It has been reported that the high Nb containing Ti_3Al can exceed Ni base alloys such as INCO 718 in specific strength and stress rupture properties over temperature range 823-973K [4, 5]. However, the mechanisms of Nb improving the oxidation resistance of Ti_3Al

has already not clear. In high temperature environment, the oxidation resistance is closely related to diffusion. Hence, it is essential to understand the diffusion behavior in Ti$_3$Al-Nb system in detail.

In Ti-Al system, two compounds, α_2-Ti$_3$Al (D019) and γ-TiAl (L10), are of great interest. Some researches on diffusion in α_2-Ti$_3$Al have been published. Riising investigated titanium self-diffusion and interdiffusion in intermetallic phase α_2-Ti$_3$Al [6]. Breuer et al. measured the trace diffusion coefficient of Ni, Fe and Nb in single-phase α_2-Ti$_3$Al to reveal the interstitial and substitutional diffusion of metallic solutes in Ti$_3$Al [7]. However, the detailed information such as the main interdiffusion coefficient for each element and the effect of diffusion behavior by containing different elements in Ti$_3$Al were not evaluated. In this study, the single-phase interdiffusion behavior in Ti$_3$Al–Nb ternary system was identified through the Ti$_3$Al/Ti$_3$AlNb diffusion couple to understand the diffusion mechanism and thus provide basis for oxidation-resistant design.

2. Experimental procedure

In our present work, single-phase α_2 alloys Ti-30Al and Ti-28.5Al-3.5Nb (at.%) ingots were prepared by arc melting using titanium sheet (>99.8 wt.% purity), aluminum sheet (>99.9 wt.% purity) and Nb bars (>99.5 wt.% purity) under Ar-atmosphere and were remelted several times to ensure adequately homogeneity. These alloys were homogenized at 1273 and 1423 K for 100h respectively, which were checked by X-ray diffraction and scanning electron microscopy (SEM) via energy-dispersive X-ray analysis to ensure that both alloys were single phase (α_2). Meanwhile, they were cut into blocks with approximate dimensions of $4 \times 4 \times 3$ mm^3 for diffusion couples and each piece of the plane of 4×4 mm^2 was ground down by water to 3000 grit and polished with 0.3 μm alumina powders.

These alloys were combined with a constant load of 5 MPa in a vacuum furnace at 1323 K for 3 h, and then sealed under pure Ar atmosphere in silicon tubes for the actual diffusion annealing. These couples were annealed at the temperatures of 1323, 1373 and 1423 K for 120h. The concentration-distance profiles for each component were measured by electron microprobe analysis (EPMA, JXA-8100, JEOL, Japan). Every measured concentration was the average value of four points in a vertical line. For further calculation, the data points were smoothed and fitted by Boltzmann function.

3. Determination of interdiffusion coefficients

In ref. [8-10], a new ternary diffusion theory was provided by Dayanada, the main and cross interdiffusion coefficients in the ternary system can be easily calculated by the measured concentrate in the same diffusion couple. The core equation of this method may be written as follow [11]:

$$\int_{x_1}^{x_2} \tilde{J}_i dx = \bar{\tilde{D}}_{i1}^3 \left[C_1(x_1) \cdot C_1(x_2) \right] + \\ + \bar{\tilde{D}}_{i2}^3 \left[C_2(x_1) \cdot C_2(x_2) \right] \qquad (1)$$

$$\int_{x_1}^{x_2} \tilde{J}_i(x \cdot x_0^{'}) dx = \\ = 2t \left\{ \bar{\tilde{D}}_{i1}^3 \left[\tilde{J}_1(x_1) - \atop \tilde{J}_1(x_2) \right] + \bar{\tilde{D}}_{i2}^3 \left[\tilde{J}_2(x_1) - \atop \tilde{J}_2(x_2) \right] \right\} \qquad (2)$$

Here, *'t'* is the diffusion annealing time, x_0' is the coordinate of Matano plane of components of 1 and 2. In a ternary alloy system, the flux of the *i*-th component, $\tilde{J}_i$, can be taken from by Fick's law.

$$\tilde{J}_i = -\tilde{D}_{i1}^3 \frac{\partial C_1}{\partial x} - \tilde{D}_{i2}^3 \frac{\partial C_2}{\partial x} \ (i=1,2) \tag{3}$$

To ensure the convenience of calculation, Eq.3 can be transformed to relative concentration variable $Y_i(x)$, by the relation (4):

$$Y_i = \frac{C_i - C_i^+}{C_i^- - C_i^+} \tag{4}$$

where C_i^+ and C_i^-, are the terminal concentrations of i at x→+∞ and -∞, respectively.

Then the Eq.5 can be written by

$$\tilde{J}_i(x^*) = \frac{(C_i^- - C_i^+)}{2t} \cdot$$
$$\cdot \left[Y_i^* \int_{-\yen}^{x^*} (1-Y_i)dx + (1-Y_i^*)\int_{x^*}^{+\yen} Y_i dx \right] \tag{5}$$
$$(i=1,2,\ldots n)$$

As a result, the main and cross interdiffusion coefficients $\tilde{D}_{ij}^{(n)}$ in this single phase couple can be calculated. (when i=j $\tilde{D}_{ij}^{(n)}$ refers to the main interdiffusion, otherwise is cross-interdiffusion coefficient).

Without regret to the concentration effect on the interdiffusion coefficient, the average ternary interdiffusion coefficients defined by Eq.6 over the selected composition range were investigated in this study [11].

$$\overline{\tilde{D}}_{ij}^3 = \frac{\int_{C_i(x^-)}^{C_i(x^+)} \tilde{D}_{ij}^3 dC_i}{\int_{C_i(x^-)}^{C_i(x^+)} dC_i} \tag{6}$$

4. Results and discussion

4.1 The fitted curve and diffusion fluxes

To resolve the constant $\overline{\tilde{D}}_{ij}^{(3)}$ in second Fick's law, Cermak and Rothova [12-13] recommended a new method to redistribution the concentration-penetration curve, thus, the concentration-dependent $\overline{\tilde{D}}_{ij}^{(3)}$ can easily calculate. As mentioned before, Boltzmann function was apply to fitted the concentration–distance profiles, then 1.76μm of internal distance in x_1 and x_2 is finally determined for this study.

Figure 1a provides a typical annealed interface micrograph measured by SEM. In the Kirkendall interface, the Kirkendall effect or Kirkendall holes were hardly visible as illustrated. Profiles for the diffusion-couple annealed at 1423 K for 120h are presented in Figure 1b–d. The average Matano planes for all components in Ti_3Al-Nb system are illustrated in these symmetric profiles. It is also indicated that the diffusion zone is less than 200 μm after the long diffusion time at high temperature. The slight deviation between the Matano plane and Kirkendall interface of this system may be generated by the size difference of the diffusion atoms.

The fluxes $\tilde{J}_i$ can be obtained easily by the concentration profile data in Figue.1 for the couple annealed at 1423 K. The profiles of interdiffusion fluxes $\tilde{J}_i$ calculated by Eq.5 for Al, Ti and Nb as a function of the distance, x. The results are shown in Figure 2. It is essential to account for the equilibrium in diffusion total flux by summing up the interdiffusion fluxes $\tilde{J}_i$ of Ti, Al and Nb [14-15].
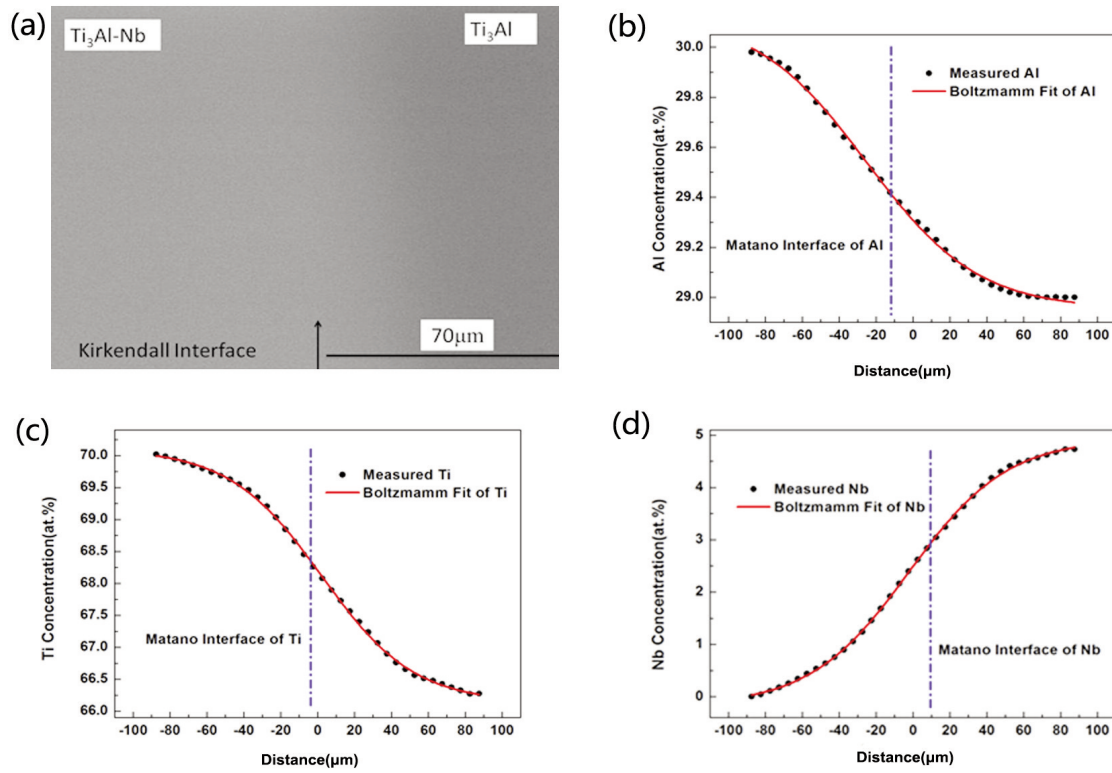
Fig 1. (a) Back-scattered electron micrograph. (b-d) Concentration profiles of (b) Al, (c) Ti, and (d) Nb for the couple annealed at 1423 K for 120 h. Solid circles and solid lines represent EPMA measurements and Smoothed curves, respectively
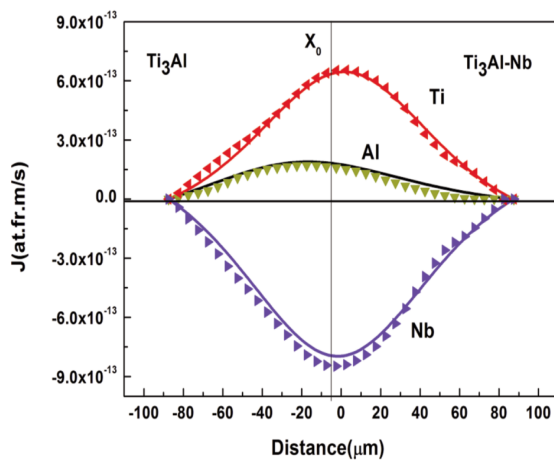

Fig 2. The corresponding interdiffusion flux profiles for a Ti₃Al/Ti₃Al-Nb diffusion couple annealed at 1423 K. Solid triangle and solid lines represent EPMA measurements and Smoothed curves, respectively.

4.2 Ternary interdiffusion coefficients

According to the analysis of Dayanada, ternary interdiffusion coefficients in Ti$_3$Al-Nb system were calculated by Eq.1-5, and the obtained results, $\tilde{D}_{NbNb}^{Al}$ and $\tilde{D}_{TiTi}^{Al}$, are indicated as example in Figure 3. Due to the numerical instability in the edge of the diffusion zone, the obtained values in the middle of the diffusion zone are plotted observably in this figure. The common features illustrated in Figure 3 are: (i) the main interdiffusion coefficients $\tilde{D}_{TiTi}^{Al}$ of in these ternary couples, are clearly larger than those of Nb; (ii) the concentration dependence of $\tilde{D}_{TiTi}^{Al}$ and $\tilde{D}_{NbNb}^{Al}$ can even be approximated by a straight line in plots of

logD vs C(Nb) changed from 0.5 to 4.0(at.%), and (iii) $\tilde{D}_{NbNb}^{Al}$ tends to increase with increasing distance that is away from the mid-diffusion zone, while $\tilde{D}_{TiTi}^{Al}$ tends to decline.
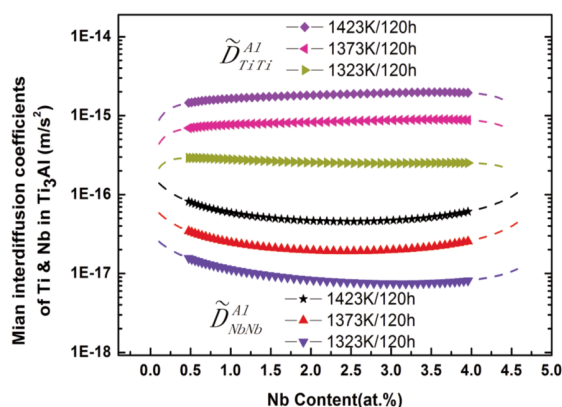

Fig 3. Concentration-dependent main interdiffusion coefficientsand $\tilde{D}_{NbNb}^{Al}$ and $\tilde{D}_{TiTi}^{Al}$ obtained from different experimental temperatures.

At the same time, the main and cross interdiffusion coefficients such as $\tilde{D}_{TiTi}^{Al}$, $\tilde{D}_{NbNb}^{Al}$, $\tilde{D}_{NbTi}^{Al}$ and $\tilde{D}_{TiNb}^{Al}$ are showed in Figure 4 where the values calculated in the middle of the diffusion zone as mentioned above. The values show the following features: (i) $\tilde{D}_{XX}^{Al}$ are concentration dependent coefficients; (ii) $\tilde{D}_{NbNb}^{Al}$ are much weaker concentration dependence than those of Ti; and (iii) relatively small non-diagonal coefficients $\left|\tilde{D}_{ij}^{Al}\right| < \left|D_{ii}^{Al}\right|$.

As shown in Figure 3, $\tilde{D}_{XX}^{Al}$ are not strongly relied on Nb concentration in the middle of the diffusion zone. Therefore, average main ternary interdiffusion coefficients defined by Eq.6 were analyzed instead, and the data calculated by this method are show in Table 1. To avoid the biased mistake in the result, the integration arrangement was
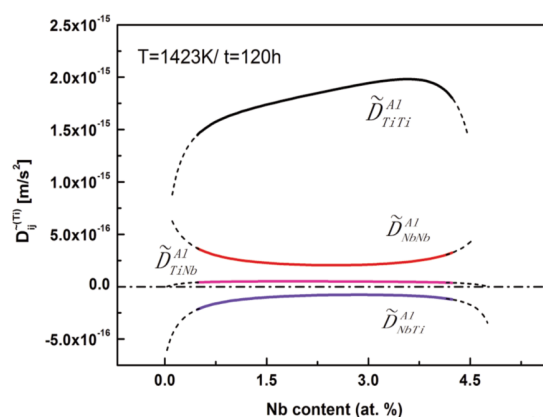

Fig 4. Concentration-dependent main and cross interdiffusion coefficients $\tilde{D}_{NbNb}^{Al}$, $\tilde{D}_{TiTi}^{Al}$, $\tilde{D}_{NbTi}^{Al}$ and $\tilde{D}_{TiNb}^{Al}$ obtained at 1423 K.

chosen in the middle of the diffusion zone according to Fig. 3 [16].

The average interdiffusion coefficients in this system, calculated from different equations sets, show some slight deviations from each other. However, they have a common trend that the interdiffusion coefficients of Nb are 20-50 times lower than the main coefficients of Ti and Al. A relationship, $\bar{\tilde{D}}_{AlAl}^{Ti} = (0.2 \sim 0.5)\bar{\tilde{D}}_{TiTi}^{Al}$, according to the calculated results, have also been illustrated. Several research on the intrinsic diffusion and self-diffusion coefficients of Al and Ti in Ti$_3$Al phase show that the proportion in this work is a little bigger than that of Rüsing and Herzig [6]. Such difference existed between them is probably caused by the facilitation brought by Nb on the diffusion behavior of Al in the Ti$_3$Al–Nb system.

By averaging $\bar{D}_{NbNb}^{Al}$ and $\bar{D}_{NbNb}^{Ti}$, the main interdiffusion coefficients of Nb and Ti in Ti$_3$Al are obtained easily, and these values are plotted against reciprocal of absolute temperature in Figure 5, together with the trace coefficients of some of the other

Table 1. Average ternary interdiffusion coefficient in α$_2$-Ti$_3$Al-Nb (10^{-18} m^2/s).

Diffusion system	Temperature	$\bar{\tilde{D}}_{NbNb}^{Al}$	$\bar{\tilde{D}}_{NbNb}^{Ti}$	$\bar{\tilde{D}}_{TiTi}^{Al}$	$\bar{\tilde{D}}_{AlAl}^{Ti}$	$\bar{\tilde{D}}_{NbTi}^{Al}$	$\bar{\tilde{D}}_{TiNb}^{Al}$
Ti$_3$Al /T3Al-Nb	1423K/120h	84.9	47.9	2467.66	1587.2	-133.7	43.9
	1373K/120h	40.2	24.7	1129	415.1	-72	26.3
	1323K/120h	14.1	8.13	357.3	66.01	-28	11

elements (Ni, Fe) in this alloy. Also, the interdiffusion coefficients of Ti in ref. [6] are plotted in this figure. The ternary interdiffusion coefficients of Ti obtained in the present work are smaller than the results measured by Breuer's method [6]. According to Dayanada's theories, the probably reason for the deviation is that the Nb doped in Ti$_3$Al system lead to the interaction among Al, Ti and Nb, thus the interdiffusion coefficients of Ti are decreased.

The summarized results in Figure 5 indicate that the diffusion of Nb in Ti$_3$Al is slow. The reason is that Nb atoms are considered to occupy Ti sites in Ti$_3$Al, the exchanges with vacancies on Ti sublattice played a leading role in the diffusion of Ti$_3$Al [17].
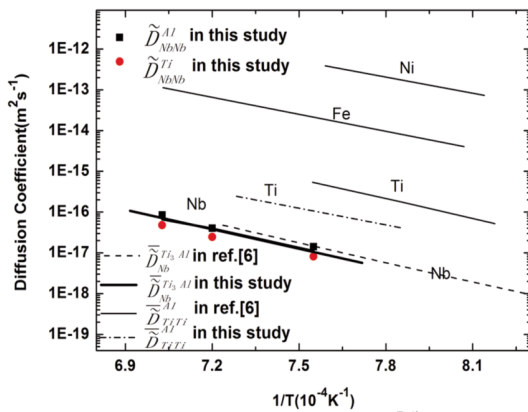

Fig 5. Comparison of the measured interdiffusion coefficients $\bar{\tilde{D}}_{Nb}^{Ti_3Al}$ with data from the literature.

4.3 Estimation of tracer diffusivities and Arrhenius parameters

In ternary alloys system, the cross-interdiffusion coefficients $\tilde{D}_{ki}^i$ and $\tilde{D}_{kj}^j$ may be negligible at infinite dilution, the tracer diffusion coefficient $\tilde{D}_k^*$ can be obtained by the value of the main coefficients $\tilde{D}_{kk}^i$ or $\tilde{D}_{kk}^j$ of impurity element [18]. Moreover, according to Cermak and Rothova's analysis, the interdiffusion coefficient $\tilde{D}_{kk}^i$ can be expressed in terms of the tracer diffusion coefficient D$_i$. By this measured method, one can write for diagonal elements $\tilde{D}_{kk}^i$:

$$\bar{\tilde{D}}_{NbNb}^{Al} = [D_{Nb}^* + c_{Nb}(D_{Al}^* - D_{Nb}^*) \cdot \\ \cdot \Phi_{NbNb}(D_{Ti}^* - D_{Al}^*)\Phi_{TiNb}] \quad (7)$$

$$\bar{\tilde{D}}_{TiTi}^{Al} = [D_{Ti}^* + c_{Ti}(D_{Al}^* - D_{Ti}^*) \cdot \\ \cdot \Phi_{TiTi}(D_{Nb}^* - D_{Al}^*)\Phi_{NbTi}] \quad (8)$$

where Φ_{ij} is a thermodynamic factor defined by the thermodynamic activity of the j-th component, a$_j$, as

$$\Phi_{ij} = c_i \left(\frac{\partial \ln a_j}{\partial c_i} \right)_{P,T,c_k \neq i} \quad (9)$$

It can be easily known with Eq.9 that when c$_x \to 0$, the Eq.7 gives $\bar{\tilde{D}}_{NbNb}^{Al} = D_{Nb}^*$ and $\bar{\tilde{D}}_{TiTi}^{Al} = D_{Ti}^*$.

The tracer interdiffusion coefficients of Nb can be extrapolated by the main interdiffusion coefficients in the ternary couples, and these   diffusion data of

Ti$_3$Al–Nb alloy at the infinite dilution of component Nb. Also, the data of tracer of lnNb are plotted against reciprocal of absolute temperature in Figure 6. These coefficients satisfy the Arrhenius equation, hence, the diffusion activation energy (Q) of Nb in Ti$_3$Al is determined from plots of logD vs 1/T and the estimated tracer interdiffusion coefficients can be written as:

$$D^*_{Nb} = 1.21 \times 10^{-4} \exp[-299.39$$
$$(kJ/mol/RT)]m^2 s^{-1} \quad (10)$$

For comparison, the results on Ti self-diffusion in Ti$_3$Al are also described previous study, which was written by [6]

$$D^*_{Ti} = (2.44^{+1.81}_{-1.04}) \times 10^{-5} \exp[-288.2 \pm 5.7$$
$$(kJ/mol/RT)]m^2 s^{-1} \quad (11)$$

The diffusion activation energy of Nb in Ti$_3$Al in this paper, 299.39 kJ/mol, is a little different from other calculated results [6]. The difference of about10 kJ/mol in the diffusion activation energy between Nb tracer-diffusion and Ti self-diffusion most probably results from an increase in the

Fig 6. Arrhenius plot of the tracer diffusion coefficients D^*_{Nb} extrapolated in Ti$_3$Al from the ternary couples in this study and the data from literature.

formation energy of vacancies in the neighborhood of Nb atoms.

These interdiffusion coefficients calculated in this study provide the research basis to understanding the diffusion behavior in Ti$_3$Al–Nb alloys. As the previous reported, when Nb is in solid solution with Ti$_3$Al, the oxidation resistance of the alloy can be improved by the addition of Nb [19-20]. According to the obtained results in this study and previous results, the interdiffusion coefficients of Ti at 1423 K in Ti$_3$Al-Nb and Ti$_3$Al system are 3.57×10^{-16} m^2/s and 4.83×10^{-16} m^2/s, respectively. Compared with the interdiffusion coefficients of Ti in Ti$_3$Al system, the interdiffusion coefficients of Ti in Ti$_3$Al-Nb system are decreased after addition of Nb into Ti$_3$Al. Moreover, the diffusion activation energy of Nb is a little bigger than that of Ti self-diffusion, which enable Nb atoms are more easily to occupy Ti sites in Ti$_3$Al, thus the diffusion of Ti is partly impeded and the size of oxide particle relatively diminished, leading to the formation of a comparatively dense and adhesive oxide with Nb doped TiO$_2$ [5]. This work contributes to investigate thermodynamic [21] and diffusion behavior in Ti-Al-Nb ternary system.

5. Conclusions

In brief, the main interdiffusion coefficients of Nb were an order of magnitude lower than that of Ti and Al in this ternary system. The interdiffusion coefficients are hardly dependent on varying concentration, in which the main interdiffusion coefficients are much larger than cross one. The interdiffusion
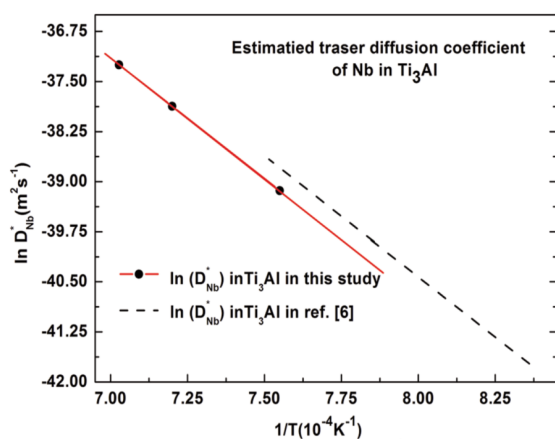
coefficients of Ti were lowered in Ti$_3$Al-Nb system compared with that in Ti$_3$Al system. The diffusion of Nb in Ti$_3$Al is extremely slow and its diffusion activation energy is 299.39 kJ/mol. The mechanisms of Nb improving the oxidation resistance of Ti$_3$Al are mainly caused by the depressed interdiffusion coefficients of Ti and the difference between Ti and Nb in activation energy.

Acknowledgement

References

[1] Kim YW, Acta Metall., 40(6) (1992) 1121.

[2] Chungen Zhou, Huibin Xu, Shengkai Gong, Kyoo Young Kim, Mater. Sci. Eng., A, 341 (1-2) (2003) 169.

[3] Yamaguchi M, Inui H, Ito K, Acta Mater., 48 (1) (2000) 307.

[4] Chu M S, Wu S K, Surf. Coat. Technol., 179 (2-3) (2004) 257.

[5] Wei Fang, Se-Hyun Ko, Hitoshi Hashimoto, Mater. Sci. Eng., A, 329-331 (2002) 708.

[6] J.Rüsing, Chr. Herzig. Intermetallics, 4 (1996) 647.

[7] J. Brever, T. Wilger, M. Friesel, Intermetallics, 7 (1999) 381.

[8] M. A. Dayananda, Metall. Mater. Trans. A, 27 (1996) 2504.

[9] M. A. Dayananda, Sohn YH, Metall. Mater. Trans. A, 30 (1999) 535.

[10] P. C. Tororici and M. A. Dayananda, Metall. Mater. Trans. A, 30 (1999) 545-550.

[11] C. Zhou, W. Gong, S. Huang, H. Wei, J. Min. Metall. Sect. B-Metall., 47 (2) (2011) 171.

[12] J. Cermak, V. Rothova, Acta Mater., 51 (1) (2003) 4411.

[13] J. Cermak, A. Gazda, V. Rothova, Intermetallics, 11 (2003) 939.

[14] R. Venkatasubramanian, M. A. Dayananda, Metall. Mater. Trans. A. 17 (1986) 362.

[15] Dengzun Yao, Junying Yang, Weiyan Gong, Chungen Zhou, Mater. Sci. Eng., A, 527 (2010) 6787.

[16] H. Wei, W. Gong, S. Huang, C. Zhou, Scripta Mater., 64 (1) (2011) 53.

[17] Y. Mishin and Chr. Herzig, Acta Mater., 48 (2000) 589.

[18] N. Garimella, M. Ode, M. Ikeda, Intermetallics, 16 (2008) 1095.

[19] Huiren Jiang, Mitsuji Hirohasi, Yun Lu, Hitoshi Imanari, Scripta Mater., 46 (2002) 639.

[20] Jim Lee, Wei Gao, Zhengwei Li, Yedong He. Mater. Lett., 57 (2003) 1528.

[21] A. Kostov, B. Friedrich, D. Živkovic, J. Mining Metall. B, 44(1) (2008) 49.